

**Preparation and Characterization of  $(i\text{PrO})_4\text{WW}(\eta^2\text{-dmpe})_2(\text{CO})$ ,  $(\eta^1\text{-O}_2\text{CH})(i\text{PrO})_4\text{WW}(\eta^2\text{-dmpe})_2(\text{H})$ ,  $[\text{H}(\eta^2\text{-dmpe})\text{W}\text{W}\text{O}_2]_2(\mu\text{-O})$ , and  $\text{W}_2(\text{O})_4(\mu\text{-O})[\text{W}(\eta^2\text{-dmpe})_2\text{CO}]_2$  (dmpe = Bisdimethylphosphinomethane), Compounds with W–W Bonds between Metal Atoms in Greatly Differing Oxidation States**

Malcolm H. Chisholm,\* Kirsten Foltg, Keith S. Kramer, and William E. Streib

Department of Chemistry and Molecular Structure Center, Indiana University, Bloomington, Indiana 47405

Received May 8, 1997

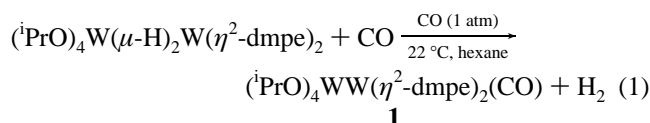
The compound  $\text{W}_2(\text{H})_2(\text{O}^i\text{Pr})_4(\eta^2\text{-dmpe})_2$  reacts in hydrocarbon solutions with CO, CO<sub>2</sub>, and H<sub>2</sub>O to give  $(i\text{PrO})_4\text{WW}(\eta^2\text{-dmpe})_2(\text{CO})$ , **1**,  $(\eta^1\text{-O}_2\text{CH})(i\text{PrO})_4\text{WW}(\eta^2\text{-dmpe})_2\text{H}$ , **2**, and  $[\text{H}(\eta^2\text{-dmpe})_2\text{W}\text{W}\text{O}_2]_2(\mu\text{-O})$ , **3**, respectively. Compound **1** reacts with H<sub>2</sub>O in hydrocarbon solvents to give  $\text{W}_2(\text{O})_4(\mu\text{-O})[\text{W}(\eta^2\text{-dmpe})_2(\text{CO})]_2$ , **4**. The compounds **1–4** contain unsupported W–W bonds between metal atoms in greatly different oxidation states. The new compounds have been characterized by NMR and infrared spectroscopy, and compounds **1** and **4**, by single-crystal X-ray studies. For **1**•0.5toluene at  $-171$  °C,  $a = 19.546(3)$  Å,  $b = 21.745(4)$  Å,  $c = 18.114(3)$  Å,  $Z = 8$ , and space group *Pcab* and for **4**•4CH<sub>2</sub>Cl<sub>2</sub> at  $-169$  °C,  $a = 13.282(2)$  Å,  $b = 14.308(3)$  Å,  $c = 15.319(3)$  Å,  $\beta = 97.88(1)^\circ$ ,  $Z = 2$ , and space group *P2<sub>1</sub>/n*.

## Introduction

Homometallic compounds with M–M multiple bonds generally contain metal atoms in similar coordination environments and oxidation states.<sup>1</sup> Exceptions are rare, and two of the more interesting examples are  $(i\text{PrO})_4\text{MoMo}(\eta^2\text{-dmpe})_2^2$  and  $\text{O}_3\text{ReRe}(\text{dmpm})_2\text{Cl}_2$ ,<sup>3</sup> wherein the oxidation states of the metal atoms differ by 4. Our recent synthesis of the compound  $(i\text{PrO})_4\text{W}(\mu\text{-H})_2\text{W}(\eta^2\text{-dmpe})_2$ <sup>4</sup> prompted us to investigate the reactions described herein, which resulted in the isolation of four new compounds,  $(i\text{PrO})_4\text{WW}(\eta^2\text{-dmpe})_2(\text{CO})$ , **1**,  $(\eta^1\text{-O}_2\text{CH})(i\text{PrO})_4\text{WW}(\eta^2\text{-dmpe})_2\text{H}$ , **2**,  $[\text{H}(\eta^2\text{-dmpe})_2\text{W}\text{W}\text{O}_2]_2(\mu\text{-O})$ , **3**, and  $[(\eta^2\text{-dmpe})_2(\text{CO})\text{W}\text{W}\text{O}_2]_2(\mu\text{-O})$ , **4**, each having an unsupported W–W multiple bond between W atoms in very different oxidation states.

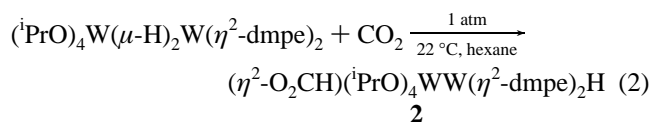
## Results

**Synthesis and Reactivity Studies.**  $(i\text{PrO})_4\text{WW}(\eta^2\text{-dmpe})_2(\text{CO})$ , **1**. Hydrocarbon solutions of  $(i\text{PrO})_4\text{W}(\mu\text{-H})_2\text{W}(\eta^2\text{-dmpe})_2$  react with CO rapidly according to eq 1. When the reaction is carried out in an NMR tube and followed by <sup>1</sup>H NMR spectroscopy, the signal for H<sub>2</sub> is observed at  $\delta$  4.66 and bubbles of H<sub>2</sub> are evolved.



The formation of **1** provides a relatively rare example of reductive elimination from a W<sub>2</sub><sup>6+</sup> center under mild conditions.<sup>5</sup> Compound **1** is obtained as a brown, air-sensitive hydrocarbon-soluble crystalline compound.

$(\eta^1\text{-O}_2\text{CH})(i\text{PrO})_4\text{WW}(\eta^2\text{-dmpe})_2\text{H}$ , **2**. The reaction between CO<sub>2</sub> and  $(i\text{PrO})_4\text{W}(\mu\text{-H})_2\text{W}(\eta^2\text{-dmpe})_2$  in hexane proceeds according to eq 2 to give the formate complex **2**, and the reaction is accompanied by a pronounced color change from brown to green.



$[\text{H}(\eta^2\text{-dmpe})_2(\text{W}\text{W}\text{O}_2)]_2(\mu\text{-O})$ , **3**. During our studies of the reactivity of  $(i\text{PrO})_4\text{W}(\mu\text{-H})_2\text{W}(\eta^2\text{-dmpe})_2$  we noticed that hydrocarbon solutions were sensitive to hydrolysis and that a color change from brown to orange occurred prior to the precipitation of orange microcrystals, **3**. This caused us to examine the reaction more closely and a stock solution of H<sub>2</sub>O in tetrahydrofuran was prepared (1.1 M). The formation of **3** proceeds ideally according to the stoichiometry shown in eq 3 though the H<sub>2</sub> elimination was not quantified. When an excess of 5 equiv of H<sub>2</sub>O is employed, a white insoluble precipitate is formed, while with less than 5 equiv some  $(i\text{PrO})_4\text{W}(\mu\text{-H})_2\text{W}(\eta^2\text{-dmpe})_2$  remains.

(5) Chisholm, M. H. *Polyhedron* **1986**, *5*, 25.

- (1) Cotton, F. A.; Walton, R. A. In *Multiple Bonds Between Metal Atoms*, 2nd ed.; Oxford University Press, Oxford, 1993.  
 (2) (a) Chisholm, M. H.; Huffman, J. C.; Van der Sluys, W. G. *J. Am. Chem. Soc.* **1987**, *109*, 2514. (b) For a detailed discussion of the bonding, see: Bursten, B. E.; Scheider, W. F. *Inorg. Chem.* **1989**, *28*, 3292.  
 (3) (a) Ara, I.; Fanwick, P. E.; Walton, W. A. *J. Am. Chem. Soc.* **1991**, *113*, 1429. (b) Ara, I.; Fanwick, P. E.; Walton, W. A. *J. Am. Chem. Soc.* **1992**, *31*, 3211.  
 (4) (a) Chisholm, M. H.; Kramer, K. S.; Streib, W. E. *Angew. Chem., Int. Ed. Engl.* **1995**, *34*, 891. (b) Chisholm, M. H.; Kramer, K. S.; Streib, W. E. *J. Am. Chem. Soc.* **1997**, *119*, 5528.

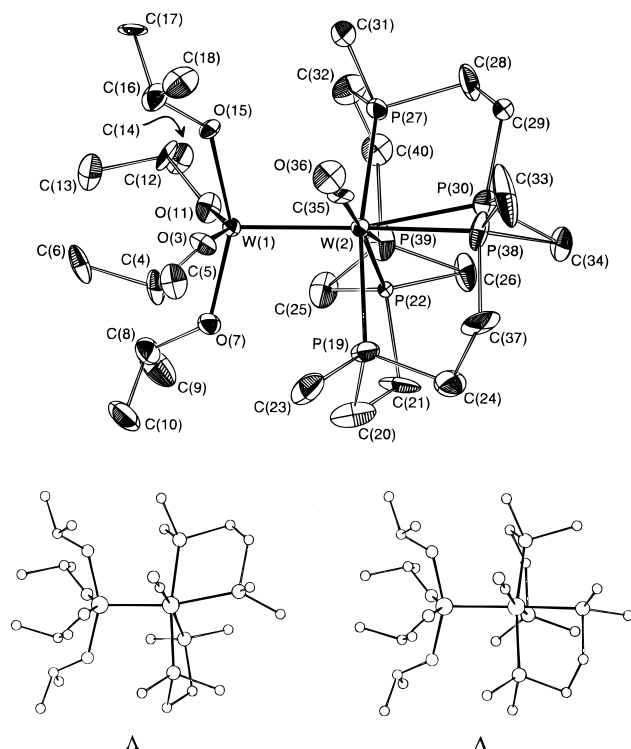
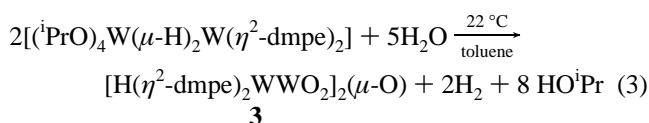


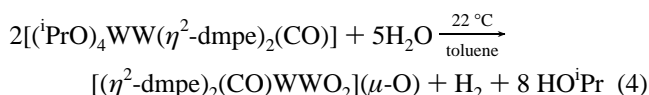
**Figure 1.** ORTEP drawing of molecule **1** giving the atom number scheme used in the table and showing the nature of the disorder of the enantiomers  $\Delta$  and  $\Delta$  because of the disposition of the  $\eta^2$ -dmpe ligands.

**Table 1.** Selected Bond Distances (deg) for  $(^i\text{PrO})_4\text{WW}(\eta^2\text{-dmpe})(\text{CO})$ , **1**

A	B	distance	A	B	distance
W(1)	W(2)	2.5242(9)	W(2)	P(30)	2.53(2)
W(1)	O(3)	1.915(9)	W(2)	P(38)	2.49(2)
W(1)	O(7)	1.939(9)	W(2)	P(39)	2.47(9)
W(1)	O(11)	1.917(9)	W(2)	C(35)	1.96(2)
W(1)	O(15)	1.945(9)	O(36)	C(35)	1.18(2)
W(2)	P(19)	2.441(4)	P	C	1.84(2) av
W(2)	P(22)	2.531(7)	O	C	1.42(1) av
W(2)	P(27)	2.430(4)			



$[(\eta^2\text{-dmpe})_2(\text{CO})\text{W}\text{W}\text{O}_2]_2(\mu\text{-O})$ , **4**. A similar hydrolysis reaction occurs for the carbonyl complex, **1** (eq 4), giving compound **4** in nearly quantitative yield due to its insolubility in nonpolar hydrocarbon solvents. The compound is, however, soluble in polar solvents such as pyridine,  $\text{CH}_2\text{Cl}_2$ , MeOH, and  $\text{H}_2\text{O}$ . The  $\text{H}_2$  evolved in eq 4 was not determined quantitatively.



**Solid-State and Molecular Structures.**  $(^i\text{PrO})_4\text{WW}(\eta^2\text{-dmpe})_2(\text{CO})$ , **1**. The solid-state molecular structure of the thermodynamic isomer of **1** (see later) is shown in Figure 1, and selected bond distances and bond angles are given in Tables 1 and 2, respectively. From the view shown in Figure 1 it is evident that the chelating dmpe ligands give rise to two enantiomers, which create disorder in the solid-state structure. Atoms C(21), P(22), C(29), and P(30) are unique to enantiomer

**Table 2.** Selected Bond Angles (deg) for  $(^i\text{PrO})_4\text{WW}(\eta^2\text{-dmpe})_2(\text{CO})$ , **1**

A	B	C	angle	A	B	C	angle
W(2)	W(1)	O(3)	101.7(3)	P(19)	W(2)	C(35)	94.4(4)
W(2)	W(1)	O(7)	103.5(3)	P(22)	W(2)	P(27)	96.3(2)
W(2)	W(1)	O(11)	108.6(3)	P(22)	W(2)	P(30)	95.8(4)
W(2)	W(1)	O(15)	102(3)	P(22)	W(2)	P(38)	97.8(4)
O(3)	W(1)	O(7)	89.2(4)	P(22)	W(2)	P(39)	21.5(3)
O(3)	W(1)	O(11)	149.6(4)	P(22)	W(2)	C(35)	170.4(4)
O(3)	W(1)	O(15)	86.4(4)	P(27)	W(2)	P(30)	77.6(3)
O(7)	W(1)	O(11)	85.4(4)	P(27)	W(2)	P(38)	92.1(4)
O(7)	W(1)	O(15)	154.3(4)	P(27)	W(2)	P(39)	75.2(3)
O(11)	W(1)	O(15)	85.7(4)	P(27)	W(2)	C(35)	93.2(4)
W(1)	W(2)	P(19)	94.0(1)	P(30)	W(2)	P(38)	14.9(3)
W(1)	W(2)	P(22)	96.9(2)	P(30)	W(2)	P(39)	95.1(4)
W(1)	W(2)	P(27)	95.27(9)	P(30)	W(2)	C(35)	85.2(6)
W(1)	W(2)	P(30)	166.0(4)	P(38)	W(2)	P(39)	102.3(4)
W(1)	W(2)	P(38)	162.7(3)	P(38)	W(2)	C(35)	80.8(5)
W(1)	W(2)	P(39)	94.6(2)	P(39)	W(2)	C(35)	168.0(5)
W(1)	W(2)	C(35)	83.2(4)	W(1)	O(3)	C(4)	138.0(9)
P(19)	W(2)	P(22)	76.0(2)	W(1)	O(7)	C(8)	128.1(9)
P(19)	W(2)	P(27)	168.6(1)	W(1)	O(11)	C(12)	132.9(8)
P(19)	W(2)	P(30)	94.7(3)	W(1)	O(15)	C(16)	130.9(9)
P(19)	W(2)	P(38)	80.8(4)	W(2)	C(35)	O(36)	179(1)
P(19)	W(2)	P(39)	97.5(3)				

$\Delta$  ( $\Delta$ ) and have half-weight while C(37), P(38), P(39), and C(40) are unique to enantiomer B ( $\Delta$ ) and also have half-weight. All other atoms are common to both enantiomers. The ball-and-stick drawings at the bottom of Figure 1 show both enantiomers, separately. The molecule contains an unsupported W–W bond of distance 2.52 Å between two very different W atoms. One is  $\text{W}^{4+}$  being bound to four O<sup>i</sup>Pr ligands in a planar arrangement, W–W–O = 104° (av), while the other tungsten is in oxidation state zero being bound to two  $\eta^2$ -dmpe ligands and one CO ligand. The CO ligand is cis to the W–W bond with W–W–C = 83°, less than 90°. This allows for a mixing of M–M and M–CO  $\pi$  bonding in a manner similar to that seen in  $\text{W}_2(\text{CO})_2(\text{OCMe}_2\text{CF}_3)_6$ .<sup>6</sup> The coordination geometry about W(2) is that of a distorted octahedron where the  $d^2$ -W(1) center occupies a single site and provides two electrons for M–M bonding. The  $d^6$ -W(2) center can thus  $\pi$  back-bond to CO with two of its  $d_\pi$  orbitals, which are with respect to the M–M bond of  $\delta$  and  $\pi$  symmetry. One  $d_\pi$  orbital on W(2) cannot back-bond to the CO ligand and is used to form a  $\pi$ -bond to W(1). In this way the M–M bond can be viewed as a double bond or alternatively as a  $d^6$ - $d^2$  M–M triple bond of the type seen in  $\text{Mo}_2(\text{O}^i\text{Pr})_4(\text{dmpe})_2$ <sup>7</sup> where one Mo–P bond is hypothetically substituted by a CO ligand which drains electron density from one of the M–M  $\pi$  bonds. The value of  $\nu(\text{CO}) = 1827\text{ cm}^{-1}$  (1784  $\text{cm}^{-1}$  for the  $^{13}\text{C}$  isotopomer) is indicative of extensive back-bonding.

$[(\eta^2\text{-dmpe})_2(\text{CO})\text{W}\text{W}\text{O}_2]_2(\mu\text{-O})$ , **4**. The solid-state molecular structure of  $[(\eta^2\text{-dmpe})_2(\text{CO})\text{W}\text{W}\text{O}_2]_2(\mu\text{-O})$ , **4**, is shown in Figure 2, and selected bond distances and angles are given in Tables 3 and 4, respectively. It is a centrosymmetric molecule with W(2) being bonded to two terminal oxo ligands, 1.73 Å (av), a  $\mu$ -oxo ligand, 1.89 Å, and W(1), W(2)–W(1) = 2.65 Å in a pseudotetrahedral manner. The W(2) coordination is akin to the W(CO)(dmpe)<sub>2</sub> moiety seen in **1** with W(2)–W(1)–C = 73°. The coordination about W(2) is that of a distorted

(6) Budzichowski, T. A.; Chisholm, M. H.; Tiedtke, D. B.; Huffman, J. C.; Streib, W. E. *Organometallics* **1995**, *14*, 2318.

(7) A reviewer raised the interesting point that, because the MO shown in **A** is primarily oxygen in character and will lie below the d block, the configuration could be  $[(d_\pi-d_\pi)ab]^2[(d_\pi-\text{O}p-d_\pi)^*]^0$ . We agree that this description may well reflect a better approximation based on orbital energetics.

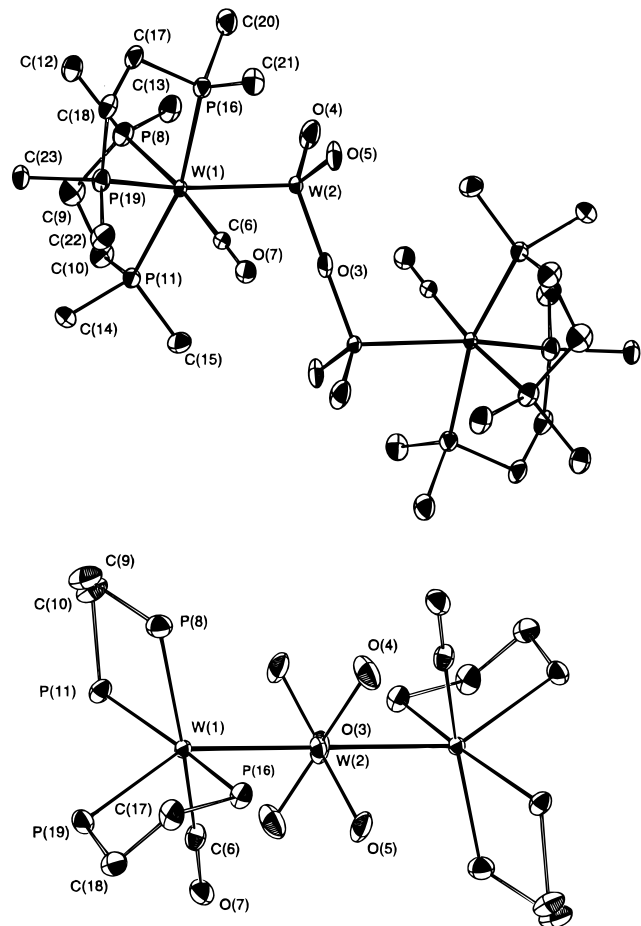


**Figure 2.** Two ORTEP drawings of molecule **4** giving the atom number scheme used in the tables.

**Table 3.** Selected Bond Distances for [(η<sup>2</sup>-dmpe)<sub>2</sub>(CO)W<sub>2</sub>O<sub>2</sub>]<sub>2</sub>(μ-O), **4**

A	B	distance	A	B	distance
W(1)	W(2)	2.6476(6)	W(2)	O(3)	1.8868(4)
W(1)	P(8)	2.524(2)	W(2)	O(4)	1.738(5)
W(1)	P(11)	2.468(2)	W(2)	O(5)	1.729(5)
W(1)	P(16)	2.467(2)	O(7)	C(6)	1.183(8)
W(1)	P(19)	2.509(2)	P	C	1.84(1) av
W(1)	C(6)	1.949(7)			

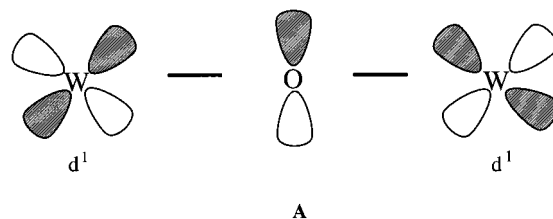
**Table 4.** Selected Bond Angles for [(η<sup>2</sup>-dmpe)<sub>2</sub>(CO)W<sub>2</sub>O<sub>2</sub>]<sub>2</sub>(μ-O), **4**

A	B	C	angle	A	B	C	angle
W(2)	W(1)	P(8)	108.15(5)	P(16)	W(1)	P(19)	77.11(6)
W(2)	W(1)	P(11)	110.39(5)	P(16)	W(1)	C(6)	98.1(2)
W(2)	W(1)	P(16)	83.08(5)	P(19)	W(1)	C(6)	84.7(2)
W(2)	W(1)	P(19)	147.48(5)	W(1)	W(2)	O(3)	110.8(2)
W(2)	W(1)	C(6)	72.8(2)	W(1)	W(2)	O(4)	111.6(2)
P(8)	W(1)	P(11)	79.87(7)	W(1)	W(2)	O(5)	108.1(2)
P(8)	W(1)	P(16)	89.88(7)	O(3)	W(2)	O(4)	111.2(2)
P(8)	W(1)	P(19)	97.44(6)	O(3)	W(2)	O(5)	108.4(2)
P(8)	W(1)	C(6)	172.0(2)	O(4)	W(2)	O(5)	106.6(3)
P(11)	W(1)	P(16)	165.02(6)	W(2)	O(3)	W(2)'	180.0
P(11)	W(1)	P(19)	93.30(6)	W(1)	C(6)	O(7)	177.8(6)
P(11)	W(1)	C(6)	92.4(2)				

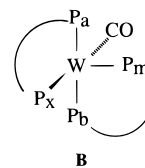
octahedral geometry where W(2) occupies one site. The oxidation states of the metal atoms are clearly zero and +5 for W(2) and W(1), respectively.

The compound gives unshifted, well-resolved NMR spectra, suggesting that it is diamagnetic. We propose that the diamagnetism arises because of three-center Wdπ-Opπ-Wdπ interactions such as that shown in **A**. This gives rise to a π<sub>b</sub><sup>2</sup>π<sub>nb</sub><sup>2</sup> MO

configuration.<sup>7</sup> The central O<sub>2</sub>WOWO<sub>2</sub> unit is similar to that seen in Cp\*(O)<sub>2</sub>WOW(O)<sub>2</sub>Cp\*.<sup>8</sup>



**Spectroscopic Studies.** (iPrO)<sub>4</sub>WW(η<sup>2</sup>-dmpe)<sub>2</sub>(CO), **1**. The <sup>1</sup>H NMR spectrum of **1** shows one O<sup>i</sup>Pr ligand and eight P<sup>i</sup>Me doublets consistent with rapid rotation about the W-W bond and a stereochemically rigid W(2) center. This is further supported by the <sup>31</sup>P{<sup>1</sup>H} spectrum which has four different <sup>31</sup>P nuclei giving rise to an ABMX spin system as shown in **B**.



The observed and simulated <sup>31</sup>P{<sup>1</sup>H} spectra for **1** are shown in Figure 3. The AB portion of the spectrum is attributed to the two trans phosphorus nuclei giving rise to the large J<sub>pp</sub> = 85 Hz. The spectrum is simplified by the unobservable (very small) coupling between P<sub>a</sub> and P<sub>x</sub> and P<sub>b</sub> and P<sub>m</sub>. Assignment of the P<sub>m</sub> and P<sub>x</sub> nuclei relative to P<sub>b</sub> and P<sub>m</sub> is based on the assumption that the noncoupled nuclei reside within the same ring (P-W-W = 77°) instead of between neighboring rings (P-W-P = 95°). In any event it is clear that the ligands bound to W(2) are stereochemically rigid on the NMR time scale. The <sup>13</sup>CO resonance appears at δ 224 as a doublet of a pseudoquartet, J<sup>31</sup>P-<sup>13</sup>C = 27.3 Hz (trans), 4.8 Hz (cis), flanked by satellites, J<sup>183</sup>W-<sup>13</sup>C = 158.6 Hz, of integral intensity 14%. This is consistent with expectations based on the structure of **1** shown in Figure 1.

Studies of the reaction shown as eq 1 show that an isomer of **1** is initially formed. This kinetic isomer shows one O<sup>i</sup>Pr ligand and two equivalent dmpe ligands; i.e., one <sup>31</sup>P signal but two sets of P<sup>i</sup>Me doublets due to their proximal and distal arrangement with respect to the M-M bond. The <sup>13</sup>CO signal is observed at δ 223 and is coupled to four equivalent <sup>31</sup>P nuclei, J<sup>31</sup>P-<sup>13</sup>C = 8.2 Hz, and to <sup>183</sup>W. Thus the kinetic isomer is proposed to have the CO ligand trans to the W-W bond. The conversion of the kinetic to the thermodynamic isomer of **1** takes roughly 16 h at 22 °C in benzene-d<sub>6</sub>.

[(η<sup>2</sup>-dmpe)<sub>2</sub>(CO)W<sub>2</sub>O<sub>2</sub>]<sub>2</sub>(μ-O). The magnitude of ν(CO) = 1800 cm<sup>-1</sup> (ν(<sup>13</sup>CO) = 1755 cm<sup>-1</sup>) in **4** is indicative of extensive Wdπ-COπ\* back-bonding, even more than in **1**. The <sup>1</sup>H NMR spectrum of **4** in pyridine-d<sub>5</sub> at room temperature consists of 16 doublets from δ 0.9 to 2.2 for the dmpe Me groups and the <sup>31</sup>P{<sup>1</sup>H} spectrum show two sets of 1:1:1:1 multiplets in a 60:40 ratio (each an AMXY spectrum). The <sup>13</sup>C spectrum of the <sup>13</sup>C-labeled derivative of **4** also shows two signals in the <sup>13</sup>C{<sup>1</sup>H} spectrum in the ratio 60:40 with coupling to <sup>31</sup>P and <sup>183</sup>W. We ascribe the above to the occurrence of anti and gauche rotamers about the central W-O-W axis as shown in **C**.

(8) Rau, M. S.; Kretz, C. M.; Geoffrey, G. L.; Rheingold, A. L.; Haggerty, B. L. *Organometallics* **1994**, *13*, 1634.

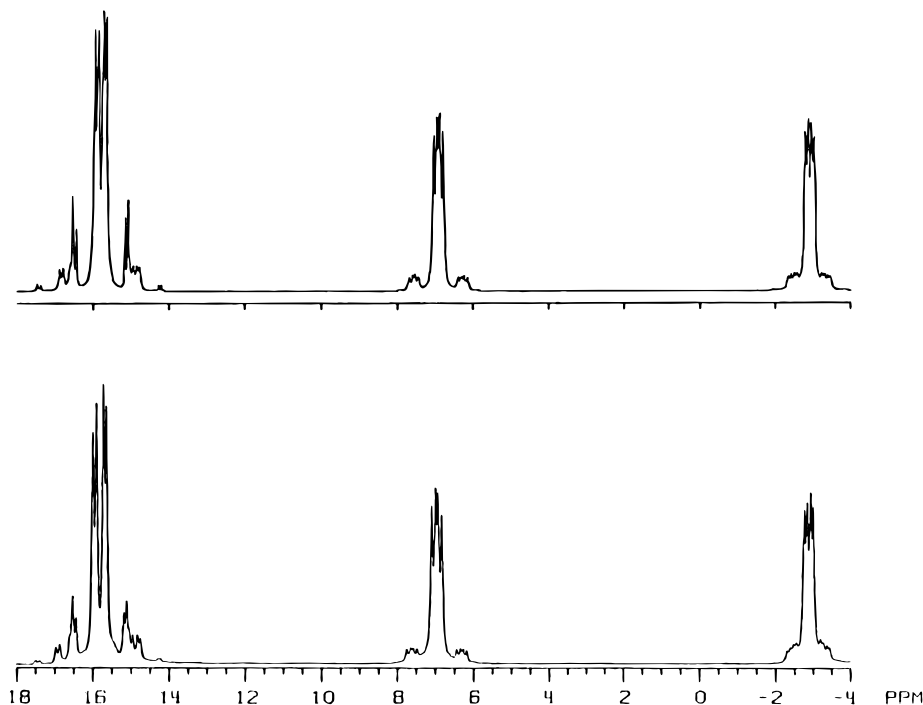
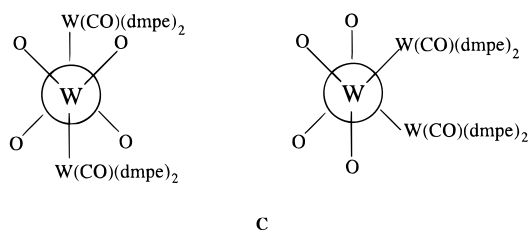
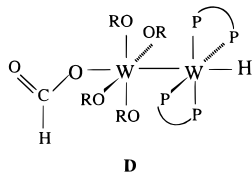


**Figure 3.**  $^{31}\text{P}\{^1\text{H}\}$  NMR spectrum of **1** in toluene- $d_8$  (bottom) and its simulated (top) ABMX pattern accompanied by satellites due to coupling to  $^{183}\text{W}$ ,  $I = 1/2$ , 14.3%. The coupling constants are (in Hz)  $J_{\text{AB}} = 85$ ,  $J_{\text{AM}} = 16$ ,  $J_{\text{AX}} = 0$ ,  $J_{\text{BM}} = 0$ ,  $J_{\text{BX}} = 13$ ,  $J_{\text{MX}} = 23.5$ ,  $J_{\text{W-P(A)}} = 260$ ,  $J_{\text{W-P(M)}} = 190.5$ , and  $J_{\text{W-P(X)}} = 130$ .



The  $^1\text{H}$  NMR spectra of **4** are relatively temperature independent from  $-30$  to  $+70$  °C in the methyl region, but from  $+80$  to  $+110$  °C the resonances collapse and broaden into eight singlets, suggesting that rotation about the central W–O–W axis is leading to anti  $\rightleftharpoons$  gauche isomerization on the NMR time scale. Finally we note that the  $^{31}\text{P}\{^1\text{H}\}$  spectra have been obtained for **4** in a variety of solvents and the ratio of the proposed rotamers has been found to be solvent dependent. In methanol- $d_4$  the two ABMX spin systems are in the ratio 80:20 while in  $\text{D}_2\text{O}$  one rotamer predominates by 95:5. This presumably reflects the influence of hydrogen bonding to the relative stabilization of gauche and anti rotamers of the type shown in **C**, which will have very different dipole moments.

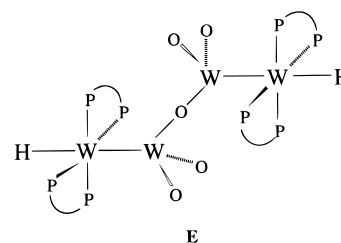
**( $\eta^1$ -O $_2$ CH)( $i$ PrO) $_4$ WW( $\eta^2$ -dmpe) $_2$ H, **2**.** The formate complex, **2**, formed by eq 2, is proposed to have the structure shown in **D**, on the basis of spectroscopic properties. The hydride



signal at  $\delta -1.58$  shows a nine line pattern whose relative intensities are consistent with a parent quintet (1:4:6:4:1) of 85.7% intensity with overlapping satellites of 14.3% intensity due to coupling to  $^{183}\text{W}$ ,  $I = 1/2$ , 14.3% natural abundance. The

$^{31}\text{P}\{^1\text{H}\}$  NMR spectrum displays one resonance at  $\delta 19.5$  flanked by tungsten satellites  $J^{183}\text{W-}^{31}\text{P} = 233$  Hz. The  $^1\text{H}$  NMR reveals two sets of  $\text{PMe}$  and  $\text{CH}_2$  doublets arising from proximal and distal groups, one  $\text{O}^i\text{Pr}$  group and a formate proton resonance at  $\delta 8.01$ . Formation of the  $^{13}\text{C}$ -labeled complex **2** employing  $^{13}\text{CO}_2$  revealed  $^1J^{13}\text{C-H} = 193$  Hz for the formate proton. The  $^{13}\text{C}\{^1\text{H}\}$  spectrum of the labeled complex showed the formate carbon signal at  $\delta 165.8$ . The seemingly only reasonable structure is once again based on a  $d^1$ - $d^5$  center (in part, related to that proposed for  $[(\text{H})(\eta^2\text{-dmpe})_2\text{W}\text{W}\text{O}_2]_2(\mu\text{-O})$  described below.

**$(\text{H})(\eta^2\text{-dmpe})_2\text{W}\text{W}\text{O}_2]_2(\mu\text{-O})$ , **3**.** Compound **3** has only been characterized spectroscopically but is proposed to be closely related to that determined for **4** in that it contains a centrosymmetric structure based on an oxo bridge as shown in **E**.



In the  $^1\text{H}$  NMR spectrum at room temperature in benzene- $d_6$ , there is a broad hydride signal at  $\delta -4.03$  and the dmpe ligands give rise to diastereotopic methyl ( $\delta 2.07$  and 1.10) and methylene resonances ( $\delta 1.80$  and 1.20) in the expected integral ratio 3:1, respectively. Furthermore, the  $^{31}\text{P}\{^1\text{H}\}$  NMR spectrum shows a single resonance  $\delta 22.2$  flanked by satellites due to coupling  $^{183}\text{W}$ ,  $J^{183}\text{W-}^{31}\text{P} = 193$  Hz. Although this is consistent with a structure akin to that shown in **E**, the location of the hydride remains uncertain.

## Concluding Remarks

The reactions of W<sub>2</sub>(H)<sub>2</sub>(O<sup>i</sup>Pr)<sub>4</sub>(dmpe)<sub>2</sub> with CO, H<sub>2</sub>O, and CO<sub>2</sub> led to products in which the segregation of hard and soft ligands is further emphasized and unsupported W–W bonds are found between metal atoms in oxidation states 0 and +4 and 0 or +1 and +5. These add to the once relatively rare group of M–M bonded compounds having metal atoms in very different oxidation states and coordination environments. That tungsten should so readily and seemingly wantonly form these types of complexes may well reflect that tungsten can be viewed as both a hard and soft metal. In its higher oxidation states it is oxophilic, while as tungsten-zero it is soft, preferring CO and phosphine ligands.

## Experimental Section

**General Procedures.** All syntheses and sample manipulations were carried out under an atmosphere of dry and deoxygenated nitrogen using standard Schlenk and glovebox techniques. Hydrocarbon solvents were distilled under N<sub>2</sub> from Na/benzophenone and stored over 4 Å molecular sieves. Spectra were recorded on Varian XL-300 (300 MHz), Nicolet NT-360 (360 MHz), and Bruker AM 500 (500 MHz) spectrometers in dry and deoxygenated benzene-*d*<sub>6</sub>, toluene-*d*<sub>8</sub>, or pyridine-*d*<sub>5</sub>. All <sup>1</sup>H NMR chemical shifts are reported in ppm relative to the residual protio impurities of the deuterated solvents. The <sup>13</sup>C NMR chemical shifts are reported relative to the carbon resonances of the solvent. <sup>31</sup>P NMR chemical shifts were calibrated against an external sample of H<sub>3</sub>PO<sub>4</sub> set at 0.0 ppm. <sup>2</sup>H NMR spectra were recorded in benzene or toluene, and the chemical shifts are reported in ppm relative to the natural abundance <sup>2</sup>H present in the protio solvent. Infrared spectra were obtained from KBr pellets or Nujol mulls using a Nicolet S10P FT-IR spectrometer. Elemental analyses were performed by Atlantic Microlab, Inc. (Norcross, GA) and Oneida Research Services (Whitesboro, NY). (PrO)<sub>4</sub>W(μ-H)<sub>2</sub>W(η<sup>2</sup>-dmpe)<sub>2</sub><sup>4</sup> was prepared as described previously.

**(PrO)<sub>4</sub>WW(η<sup>2</sup>-dmpe)<sub>2</sub>(CO), 1.** In a 20 mL capacity Kontes brand solvent seal flask, W<sub>2</sub>(μ-H)<sub>2</sub>(dmpe)<sub>2</sub>(O<sup>i</sup>Pr)<sub>4</sub> (0.200 g, 0.221 mmol) was dissolved in ca. 10 mL hexane. The solution was then frozen in liquid nitrogen and the flask evacuated. One atm of CO was added by way of a gas transfer manifold; the flask was closed, warmed to room temperature, and left stirring for 24 h. The reaction mixture was filtered transferred to a standard Schlenk flask, where the volume of solvent was then reduced to ca. 1 mL. After 3–4 days at –20 °C, brown crystals were isolated by cannulating off the mother liquor (yield: 0.190 g, 92%). Anal. Calcd (found) for W<sub>2</sub>P<sub>4</sub>O<sub>4</sub>C<sub>24</sub>H<sub>60</sub>: C, 32.21 (31.88); H, 6.49 (6.27). <sup>1</sup>H NMR (300 MHz, 22 °C, benzene-*d*<sub>6</sub>): OC(H)(CH<sub>3</sub>)<sub>2</sub>, δ 4.63 (quintet, 4H, J<sub>HH</sub> = 6.0 Hz); OC(H)(CH<sub>3</sub>)<sub>2</sub>, δ 1.56 (d, 12H, J<sub>HH</sub> = 5.7 Hz), δ 1.41 (d, 12H, J<sub>HH</sub> = 6.3 Hz); (CH<sub>3</sub>)<sub>2</sub>PCH<sub>2</sub>CH<sub>2</sub>P(CH<sub>3</sub>)<sub>2</sub>, δ 2.24 (d, 3H, J<sub>HP</sub> = 7.5 Hz), δ 2.15 (d, 3H, J<sub>HP</sub> = 7.2 Hz), 2.05 (d, 3H, J<sub>HP</sub> = 7.5 Hz), 1.86 (d, 3H, J<sub>HP</sub> = 5.1 Hz), 1.29 (d, 3H, J<sub>HP</sub> = 5.1 Hz), 1.26 (d, 3H, J<sub>HP</sub> = 6.3 Hz), 0.80 (d, 3H, J<sub>HP</sub> = 4.5 Hz), 0.47 (d, 3H, J<sub>HP</sub> = 3.6 Hz); (CH<sub>3</sub>)<sub>2</sub>PCH<sub>2</sub>CH<sub>2</sub>P(CH<sub>3</sub>)<sub>2</sub>: δ 0.50–2.0 (broad multiplets, 8H). <sup>13</sup>C{<sup>1</sup>H} (75 MHz, 22 °C, benzene-*d*<sub>6</sub>): δ 224.0 (pseudo dqt, 1C, CO, J<sup>183</sup>W–<sup>13</sup>C = 158.6 Hz, J<sup>13</sup>C–<sup>31</sup>P(trans) = 27.3 Hz, J<sup>13</sup>C–<sup>31</sup>P(cis) = 4.8 Hz, 14.3%). <sup>31</sup>P{<sup>1</sup>H} NMR (146 MHz, 22 °C, benzene-*d*<sub>6</sub>): δ 15.7 (AB quartet, 2P, dmpe), δ 6.8 (dd, 1P, dmpe), δ –3.0 (dd, 1P, dmpe), simulated coupling constants (Hz) for the ABMX pattern are J<sub>AB</sub> = 85, J<sub>AM</sub> = 16, J<sub>AX</sub> = 0, J<sub>BM</sub> = 0, J<sub>BX</sub> = 13, J<sub>MX</sub> = 23.5, J<sub>W–P(A)}</sub> = 370, J<sub>W–P(B)}</sub> = 260, J<sub>W–P(M)}</sub> = 190.5, J<sub>W–P(X)}</sub> = 130. IR (Nujol mull): ν<sub>CO</sub> = 1827 (ν<sup>13</sup>CO = 1784). IR (KBr pellet): 1804 (ν<sub>CO</sub>), 1418 w, 1370 w, 1331 w, 1273 w, 1163 s, 1121 s, 999 m, 970 s, 994 s, 889 m, 873 m, 693 w, 642 w, 586 m. Kinetic intermediate: <sup>1</sup>H NMR (300 MHz, 22 °C, benzene-*d*<sub>6</sub>): OC(H)(CH<sub>3</sub>)<sub>2</sub>, δ 4.37 (sept, 4H, J<sub>HH</sub> = 5.7 Hz); OC(H)(CH<sub>3</sub>)<sub>2</sub>, δ 1.23 (d, 24H, J<sub>HH</sub> = 5.7 Hz); (CH<sub>3</sub>)<sub>2</sub>PCH<sub>2</sub>CH<sub>2</sub>P(CH<sub>3</sub>)<sub>2</sub>, δ 2.10 (bs, 12H); δ 1.58 (bs, 12H). <sup>31</sup>P{<sup>1</sup>H} NMR (146 MHz, 22 °C, benzene-*d*<sub>6</sub>) δ 26.2 (s, 4P, J<sup>183</sup>W–<sup>31</sup>P = 272.0 Hz, 14.3%).

**(η<sup>1</sup>-O<sub>2</sub>CH)(PrO)<sub>4</sub>WW(η<sup>2</sup>-dmpe)<sub>2</sub>H, 2.** In a Schlenk flask, a ca. 5 mL toluene solution of W<sub>2</sub>(μ-H)<sub>2</sub>(dmpe)<sub>2</sub>(O<sup>i</sup>Pr)<sub>4</sub>, (0.200 g, 0.221 mmol) was frozen in liquid N<sub>2</sub>, and the flask was evacuated. On a gas transfer manifold, 1 atm of CO<sub>2</sub> was delivered to the flask. Upon warming,

the previously brown solution began to turn dark green. After stirring for 12 h the volume of the solvent was reduced to ca. 2 mL and the flask was cooled to –20 °C. Two crops of crystals were isolated (yield: 1.46 g, 70%). Anal. Calcd (found) for W<sub>2</sub>P<sub>4</sub>O<sub>6</sub>C<sub>25</sub>H<sub>62</sub>: C, 31.60 (31.29); H, 6.58 (6.18). <sup>1</sup>H NMR (300 MHz, 22 °C, benzene-*d*<sub>6</sub>): W–H, δ –1.58 (quin, 1H, J<sub>H–<sup>31</sup>P}</sub> = 18.5 Hz, J<sup>183</sup>W–<sup>31</sup>P = 73.5 Hz, 14.3%); OC(H)(CH<sub>3</sub>)<sub>2</sub>, δ 4.37 (quintet, 4H, J<sub>HH</sub> = 6.0 Hz); OC(H)(CH<sub>3</sub>)<sub>2</sub>, δ 1.27 (d, 24H, J<sub>HH</sub> = 6.0 Hz); OC(O)H, δ 8.02 (s, 1H); O<sup>13</sup>C(O)H, δ 8.02 (d, 1H, J<sup>13</sup>C–<sup>1</sup>H = 192 Hz); (CH<sub>3</sub>)<sub>2</sub>PCH<sub>2</sub>CH<sub>2</sub>P(CH<sub>3</sub>)<sub>2</sub>, δ 2.07 (bs, 12H), 1.26 (bs, 12H, overlapping with O<sup>i</sup>Pr methyl resonance); (CH<sub>3</sub>)<sub>2</sub>PCH<sub>2</sub>CH<sub>2</sub>P(CH<sub>3</sub>)<sub>2</sub>, δ 1.80 (bm, 4H), 1.53 (bm, 4H). <sup>13</sup>C{<sup>1</sup>H} (75 MHz, 22 °C, benzene-*d*<sub>6</sub>): δ 165.8 (s, O<sup>13</sup>C(O)H). <sup>13</sup>C (75 MHz, 22 °C, benzene-*d*<sub>6</sub>): δ 165.8 (d, O<sup>13</sup>C(O)H, J<sup>13</sup>C–<sup>1</sup>H = 192 Hz). <sup>31</sup>P{<sup>1</sup>H} δ 19.53 (s, 4P, J<sup>183</sup>W–<sup>31</sup>P = 233.4 Hz).

**[(H)(η<sup>2</sup>-dmpe)<sub>2</sub>WWO<sub>2</sub>]<sub>2</sub>(μ-O), 3.** To a Schlenk flask containing a 5 mL toluene solution of W<sub>2</sub>(μ-H)<sub>2</sub>(dmpe)<sub>2</sub>(O<sup>i</sup>Pr)<sub>4</sub>, **3** (0.200 g, 0.221 mmol), was added a 1.11 molar H<sub>2</sub>O solution in THF (600 μL, 0.662 mmol) by a μL syringe. After 12 h of stirring at 22 °C, the volume was reduced until microcrystalline material began to appear. The flask was then warmed gently to redissolve the precipitated product and then cooled to –20 °C. Two crops of crystals were isolated in this manner (yield: 0.115 g, 80%). <sup>1</sup>H (300 MHz, 22 °C, benzene-*d*<sub>6</sub>): M–H: δ –4.0 (bs, 2H); (CH<sub>3</sub>)<sub>2</sub>PCH<sub>2</sub>CH<sub>2</sub>P(CH<sub>3</sub>)<sub>2</sub>, δ 2.07 (bs, 24H), δ 1.10 (bs, 24H); (CH<sub>3</sub>)<sub>2</sub>PCH<sub>2</sub>CH<sub>2</sub>P(CH<sub>3</sub>)<sub>2</sub>, δ 1.80 (bs, 8H), δ 1.19 (bs, 8H). <sup>31</sup>P{<sup>1</sup>H} δ 22.19 (s, 8P, J<sup>183</sup>W–<sup>31</sup>P = 192.6 Hz).

**[(CO)(η<sup>2</sup>-dmpe)<sub>2</sub>WWO<sub>2</sub>]<sub>2</sub>(μ-O), 4.** In a Kontes brand solvent seal flask, W<sub>2</sub>(μ-H)<sub>2</sub>(dmpe)<sub>2</sub>(O<sup>i</sup>Pr)<sub>4</sub> (0.200 g, 0.221 mmol) was dissolved in ca. 10 mL toluene. One atm of CO was added to generate W<sub>2</sub>(CO)(dmpe)<sub>2</sub>(O<sup>i</sup>Pr)<sub>4</sub>, **4**, as described above. The W<sub>2</sub>(CO)(dmpe)<sub>2</sub>(O<sup>i</sup>Pr)<sub>4</sub> solution was then transferred to a standard Schlenk flask where a 1.11 molar H<sub>2</sub>O (600 μL, 0.662 mmol) solution in THF was added by μL syringe. The reaction mixture was left standing at room temperature without stirring for 24 h, whereupon orange needles were deposited on the sides of the flask. The mother liquor was removed by cannula, and the orange solid was washed twice with 5 mL of hexane and dried *in vacuo* (yield: 0.148 g, 97%). X-ray-quality crystals were grown from CH<sub>2</sub>Cl<sub>2</sub>. Anal. Calcd (found) for W<sub>4</sub>P<sub>8</sub>O<sub>7</sub>C<sub>26</sub>H<sub>64</sub>: C, 21.22 (20.83); H, 4.38 (4.43). <sup>1</sup>H NMR (500 MHz, 22 °C, pyridine-*d*<sub>5</sub>): (CH<sub>3</sub>)<sub>2</sub>PCH<sub>2</sub>CH<sub>2</sub>P(CH<sub>3</sub>)<sub>2</sub>, δ 0.90–2.23 (16 doublets consistent with the presence of two rotamers in ca. 40:60 ratio); (CH<sub>3</sub>)<sub>2</sub>PCH<sub>2</sub>CH<sub>2</sub>P(CH<sub>3</sub>)<sub>2</sub>, δ 0.90–2.00 (broadened multiplets along the baseline overlapping with the methyl resonances). <sup>31</sup>P{<sup>1</sup>H} (146 MHz, 22 °C, pyridine-*d*<sub>5</sub>): Rotamer A, δ 17.45 (dd, 1P, J<sub>PP}</sub> = 57.4 Hz, J<sub>PP}</sub> = 23.9 Hz), δ 13.09 (ddd, 1P, J<sub>PP}</sub> = 57.4 Hz, J<sub>PP}</sub> = 23.0 Hz, J<sub>PP}</sub> = 8.1 Hz), δ 7.16 (dt, 1P, J<sub>PP}</sub> = 7.8 Hz), δ 3.66 (t, 1P, J<sub>PP}</sub> = 26.4 Hz); Rotamer B, δ 16.23 (dd, 1P, J<sub>PP}</sub> = 55.9 Hz, J<sub>PP}</sub> = 25.1 Hz), δ 14.27 (ddd, 1P, J<sub>PP}</sub> = 56.4 Hz, J<sub>PP}</sub> = 21.5 Hz, J<sub>PP}</sub> = 9.3 Hz), δ 6.11 (dt, 1P, J<sub>PP}</sub> = 26.0 Hz, J<sub>PP}</sub> = 8.8 Hz), δ 4.10 (t, 1P, J<sub>PP}</sub> = 24.7 Hz). <sup>31</sup>P{<sup>1</sup>H} (146 MHz, 22 °C, D<sub>2</sub>O): δ 13.9 (m, 1P), δ 8.5 (m, 1P), δ 0.767 (m, 2P). <sup>13</sup>P{<sup>1</sup>H} (125 MHz, 22 °C, pyridine-*d*<sub>5</sub>): Rotamer A, δ 220.7 (m, 1C, CO, J<sup>183</sup>W–<sup>13</sup>C = 149.5 Hz); Rotamer B, δ 219.6 (m, 1C, CO, J<sup>183</sup>W–<sup>13</sup>C = 145.5 Hz). IR (KBr pellet, cm<sup>–1</sup>): ν<sub>CO</sub> = 1800, ν<sup>13</sup>CO = 1755, 1418 m, 1283 m, 1124 w, 922 s, 887 s, 835 m, 785 s, 727.26 m, 694 m, 644 m.

**Crystallographic Studies.** General operating procedures and listings of programs have been given previously.<sup>9</sup> A summary of crystal data is given in Table 5.

**1.0.5 Toluene.** A crystal of suitable size was mounted in a capillary in a nitrogen atmosphere glovebag by using silicone grease. The crystal was then transferred to a goniostat where it was cooled to –171 °C for characterization and data collection. A selective search of a limited hemisphere of reciprocal space revealed a primitive orthorhombic cell. Following 2-fold redundant (+*h*, +*k*, +*l*) intensity data collection, the conditions *l* = 2*n*, for *Ok**l*, *h* = 2*n* for *h0l*, and *k* = 2*n* for *hk0* uniquely determined space group *Pcab*. After correction for absorption, data processing gave a unique set of 5056 intensities and a residual of 0.058 for the averaging of 4865 of these which had been observed more than

(9) Chisholm, M. H.; Foltling, K.; Huffman, J. C.; Kirkpatrick, C. C. *Inorg. Chem.* **1984**, *23*, 1021.

**Table 5.** Summary of Crystal Data

	1	4
empirical formula	C <sub>25</sub> H <sub>60</sub> O <sub>5</sub> P <sub>4</sub> W <sub>2</sub> · 0.5C <sub>6</sub> H <sub>5</sub> CH <sub>3</sub>	C <sub>26</sub> H <sub>64</sub> O <sub>7</sub> P <sub>8</sub> W <sub>4</sub> · 4CH <sub>2</sub> Cl <sub>2</sub>
space group	<i>Pcab</i>	<i>P2<sub>1</sub>/n</i>
cell dimensions		
temperature (°C)	−171	−169
<i>a</i> (Å)	19.546(3)	13.282(2)
<i>b</i> (Å)	21.745(4)	14.308(3)
<i>c</i> (Å)	18.114(3)	15.319(3)
β (deg)		97.88(1)
Z (molecules/cell)	8	2
Volume (Å <sup>3</sup> )	7698.86	2883.71
<i>d</i> <sub>calcd</sub> (g/cm <sup>3</sup> )	1.688	2.086
wavelength (Å)	0.710 69	0.710 69
molecular wt	978.41	1811.67
linear abs coeff (cm <sup>−1</sup> )	62.955	85.898
<i>R</i> ( <i>F</i> ) <sup>a</sup>	0.0511	0.0245
<i>R</i> <sub>w</sub> ( <i>F</i> ) <sup>b</sup>	0.0453	0.0266

$$^a R(F) = \frac{\sum ||F_o| - |F_c||}{\sum |F_o|}, \quad ^b R_w(F) = \frac{\{\sum w(|F_o| - |F_c|)^2\}^{1/2}}{\sum w F_o^2}$$

once. Four standards (−6,0,0; 0,−12,0; −3,−3,−3; and 0,0,−4) measured every 300 data showed no significant trends.

The structure was solved by using a combination of direct methods (MULTAN78) and Fourier techniques. The positions of the tungsten atoms were obtained from an initial *E* map. The positions of the remaining non-hydrogen atoms were obtained from subsequent iterations of least-squares refinement and difference Fourier calculation. The structure obtained is a combination of two isomers which apparently pack equally well in the crystal. In addition the difference map contained a number of peaks near a crystallographic center of symmetry which made no chemical sense and which were assumed to be disordered solvent. Since toluene had been used as the solvent, half a molecule of toluene per asymmetric unit was used for the title formula and for the calculation of density and absorption coefficient. The occupancies of these solvent peaks refined to an average of 65%, and they were fixed at that value for the remaining cycles of refinement. Very few of the peaks could be identified as hydrogen atoms, and in view of the disordered nature of the crystal structure, no further attempt was made to include them. Atoms C(21), P(22), C(29), and P(30) are unique to Molecule A and have half-weight. Atoms C(37), P(38), P(39), and C(40) are unique to Molecule B and have half-weight. All other atoms in the two isomers are common to both isomers and have full weight. Three of these, P(22), C(29), and C(40) could not be refined anisotropically. These and the solvent peaks were refined isotropically. All other atoms were refined anisotropically to a final *R*(*F*) = 0.051 for the 371 total variables using all of the unique data.

Data having  $F < 3\sigma(F)$  were given zero weight and are indicated with asterisks in the Supporting Information of *F<sub>o</sub>* and *F<sub>c</sub>*. The largest peak in the final difference map was 1.41, and the deepest hole was −1.40 e/Å<sup>3</sup>.

**4·4CH<sub>2</sub>Cl<sub>2</sub>.** A crystal of suitable size was mounted on a glass fiber with silicone grease, and it was then transferred to a goniostat where it was cooled to −169 °C for characterization and data collection. A selective search of a limited hemisphere of reciprocal space revealed a primitive monoclinic cell. Following complete intensity data collection, the conditions  $h + 1 = 2n$  for *h*0*l* and  $k = 2n$  for 0*k*0 uniquely determined space group *P2<sub>1</sub>/n*. After correction for absorption, data processing produced a unique set of 3775 intensities and gave a residual of 0.029 for the averaging of 3450 of these which has been observed more than once. Four standards (0,6,0; 0,0,−4; −3,3,−4; and −6,0,0) measured every 300 data showed no significant trends.

The structure was solved by using a combination of direct methods (MULTAN78) and Fourier techniques. The positions of the tungsten atoms were obtained from an initial *E* map. The positions of the remaining non-hydrogen atoms were obtained from subsequent iterations of a least-squares refinement followed by a difference Fourier calculation. In addition to the half-molecule of interest, the asymmetric unit contains two molecules of CH<sub>2</sub>Cl<sub>2</sub> which had been used as solvent. Hydrogens were included in fixed calculated positions with thermal parameters fixed at one plus the isotropic thermal parameter of the atom to which they were bonded. In the final cycles of refinement, the non-hydrogen atoms were varied with anisotropic thermal parameters to give a final *R*(*F*) = 0.025 for the 263 total variables using all of the unique data. Data having  $F < 3\sigma(F)$  were given zero weight and are indicated with asterisks in the Supporting Information of *F<sub>o</sub>* and *F<sub>c</sub>*. The largest peaks in the final difference map were W(1) and W(2) residuals 1.6 and 1.4 e/Å<sup>3</sup>, all others being less than 1 e/Å<sup>3</sup>. The deepest hole was −0.7 e/Å<sup>3</sup>.

Atom O(3) of the molecule of interest lies on a crystallographic center of symmetry and the molecule therefore has four molecules of solvent associated with it.

Symmetry-related atoms in the tables and figures are indicated with primes.

**Acknowledgment.** We thank the Department of Energy, Office of Basic Sciences, Chemistry Division for financial support.

**Supporting Information Available:** X-ray crystallographic data for compounds **1** (*i*(PrO)<sub>4</sub>WW(η<sup>2</sup>-dmpe)<sub>2</sub>(CO)) and **4** [(η<sup>2</sup>-dmpe)<sub>2</sub>(CO)-WWO<sub>2</sub>]<sub>2</sub>(μ-O) are available on the Internet only. Access information is given on any current masthead page.

IC9705249